Delta-X Open Data Workshop:

Airborne Visible/Infrared Imaging Spectrometer—Next Generation Vegetation Products

Daniel Jensen

Jet Propulsion Laboratory, California Institute of Technology

June 5, 2023

Imaging Spectroscopy

- What is imaging spectroscopy/hyperspectral data?
  - Continuous radiance measurements → surface reflectance
    - "Image Cube" estimating VSWIR reflectance properties per pixel
    - Spectral characteristics associated with plant structural and biochemical properties
- Airborne Visible-Infrared Imaging Spectrometer–Next Generation (AVIRIS-NG)
  - Wavelengths: ~380 – 2500 nm
  - ~5 nm sampling
    - 425 bands
  - ~5 m spatial resolution

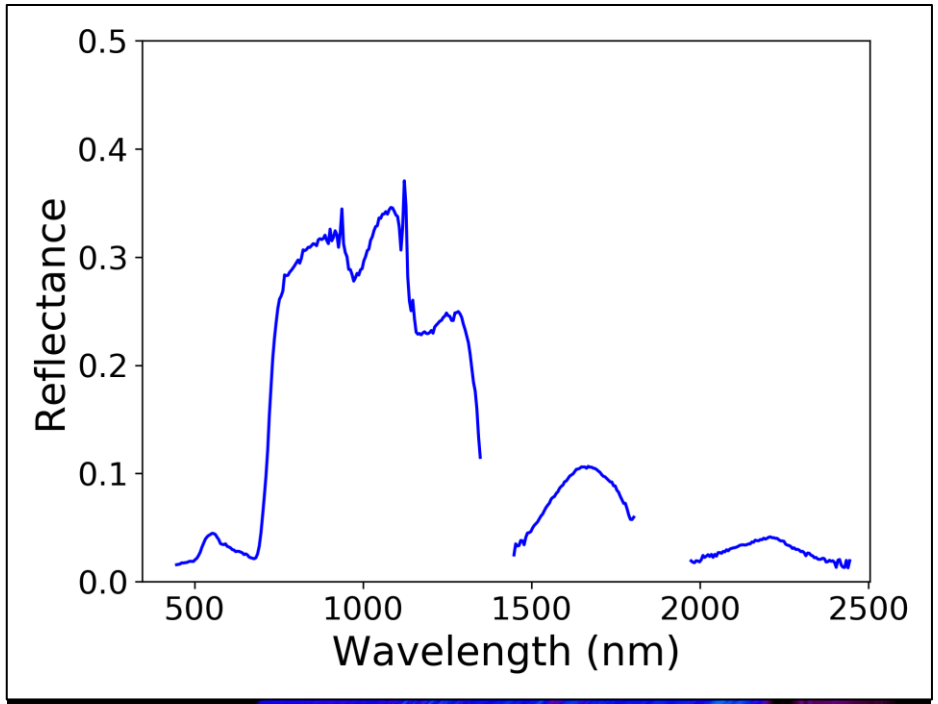

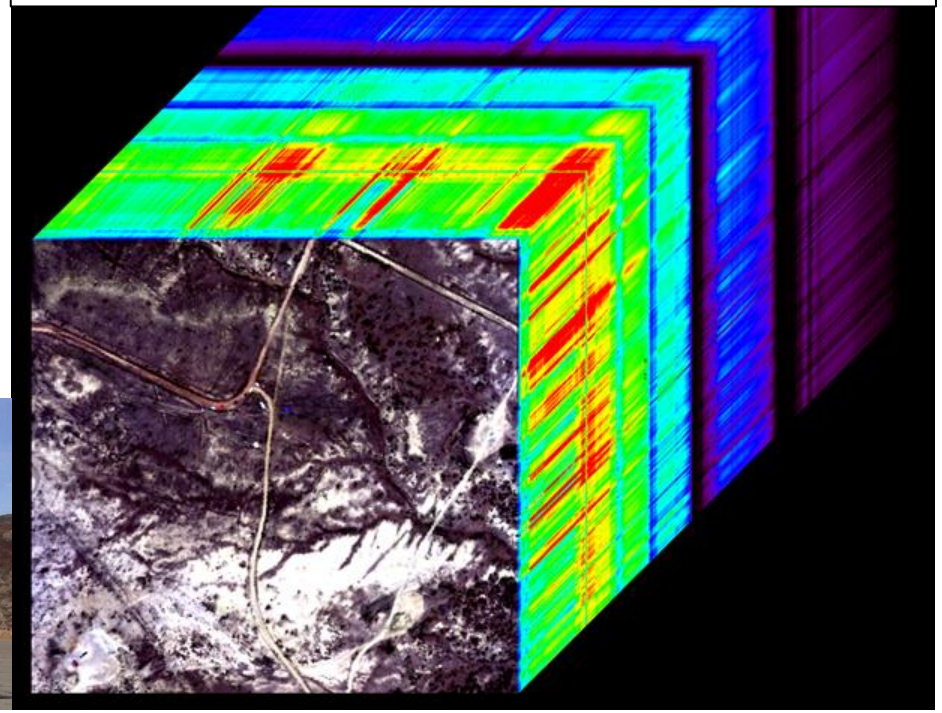

(https://aviris-ng.jpl.nasa.gov/science.html)

Airborne Visible/Infrared Imaging Spectrometer–Next Generation (L1-L3)

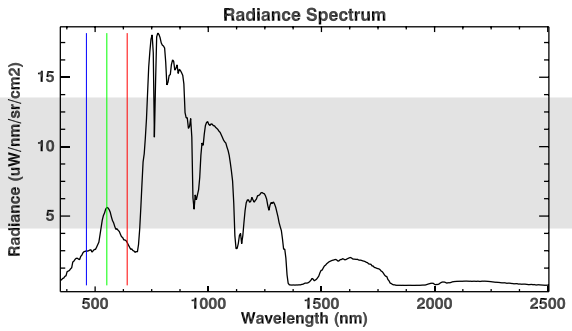

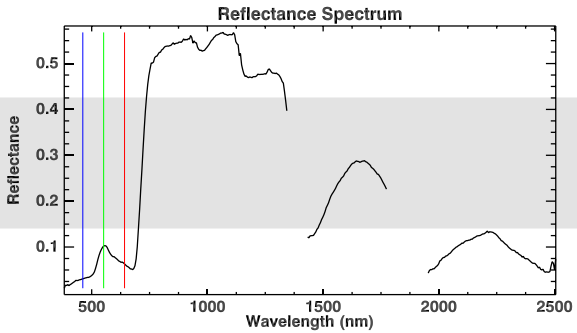

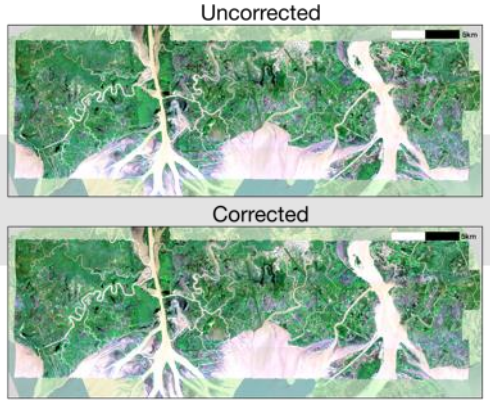

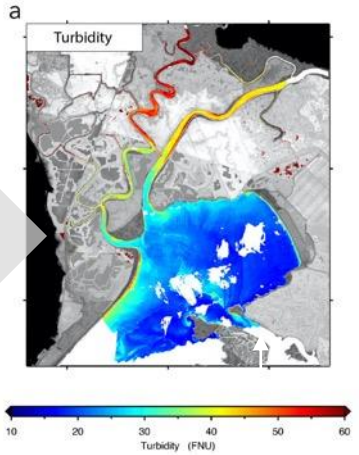

(Image courtesy of David Thompson & Evan Greenberg)

Radiance at sensor

Surface Reflectance (HRDF)

BRDF and glint correction

Vegetation and water sediment maps

- Radiance products use May 2021 hangar calibration data (Chapman et al. 2019) and atmospheric features for in-flight wavelength calibration adjustments (Thompson et al. 2015)
- Atmospheric correction is the EMIT mission approach of Optimal Estimation (Thompson et al. 2018, 2019) with speed enhancements (Thompson et al. 2020)
- BRDF correction via FlexBRDF (Queally et al., 2022) and simultaneous sunglint correction (Greenberg et al. 2022)

Delta-X AVIRIS-NG Data Products

- Spring, Fall, Post-Hurricane Ida Deployments: 144 Terrestrial Vegetation flightlines, 44 Water Quality flightlines
- L1
  - Radiance at Sensor flightlines
- L2
  - Surface Reflectance flightlines
- L2B
  - BRDF and Glint-Corrected flightlines
  - BRDF and Glint-Corrected mosaics + mask files
- L3
  - Water Quality (Suspended Sediment Concentration)
  - Vegetation Type Maps
  - Aboveground Biomass Maps

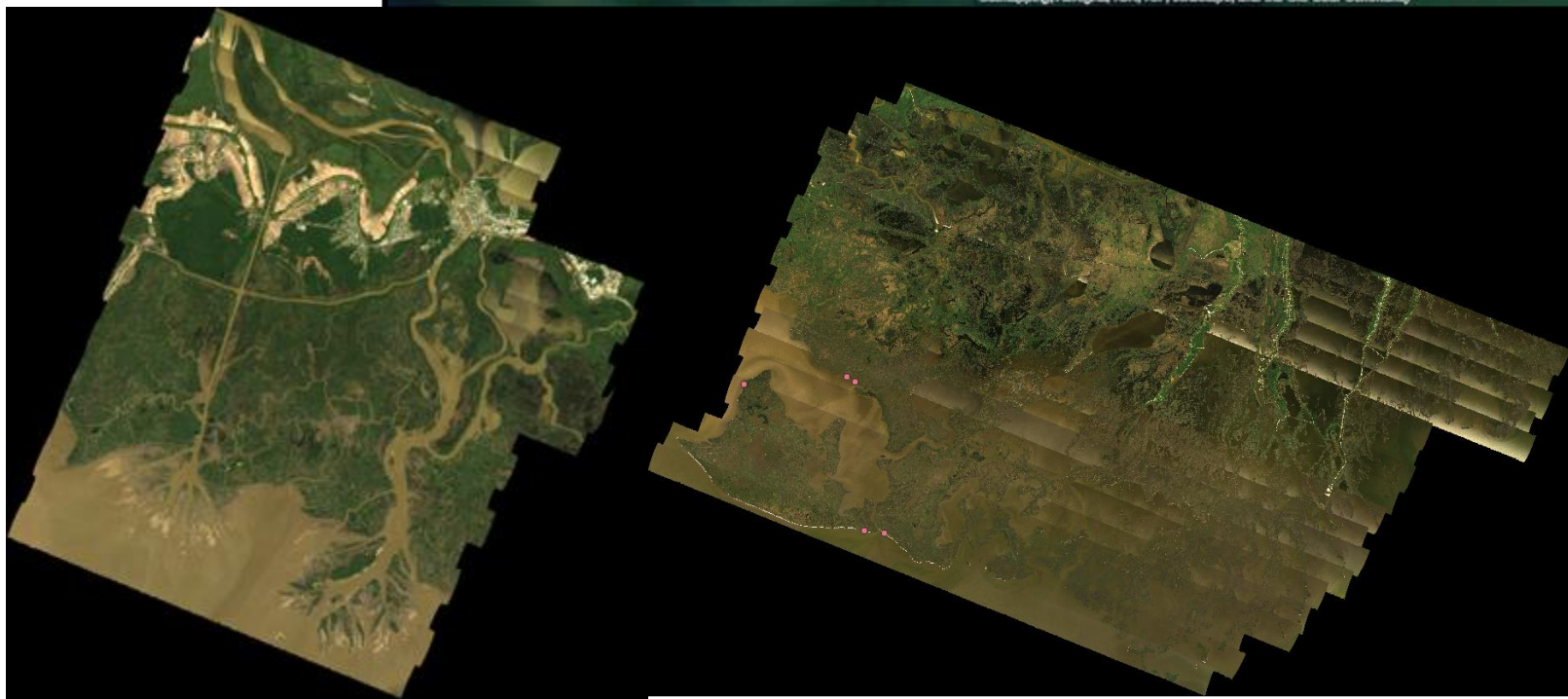

Vegetation Mapping

- Classification Scheme
  - Forest
    - *Acer rubrum, Salix nigra, Morella Cerifera, Nyssa aquatica, Triadica sebifera, Avicennia germinans*
  - Broadleaf Herbaceous
    - *Sagittaria lancifolia, Vigna luteola, Colacasia esculenta, Polygonum punctatum, Murdannia keisak, Thelypteris palustris*
  - Saltmarsh Grasses
    - *Spartina patens, Spartina alterniflora, Lythrum lineare, Spartina cynosuroides, Juncus roemarianus*
  - Freshwater Grasses
    - *Panicum hemitomon, Schoenoplectus californicus, Luziola peruviana, Eleocharis montana, Eleocharis R*
  - Tall Grasses
    - *Phragmites australis, Typha domingensis, Typha latifolia, Zizaniopsis miliacea*
  - Aquatic Vegetation (Floating/Submerged)
    - *Ludwigia grandiflora, Nelumbo lutea, Eichornia crassipes*
  - Soil/Mudflat

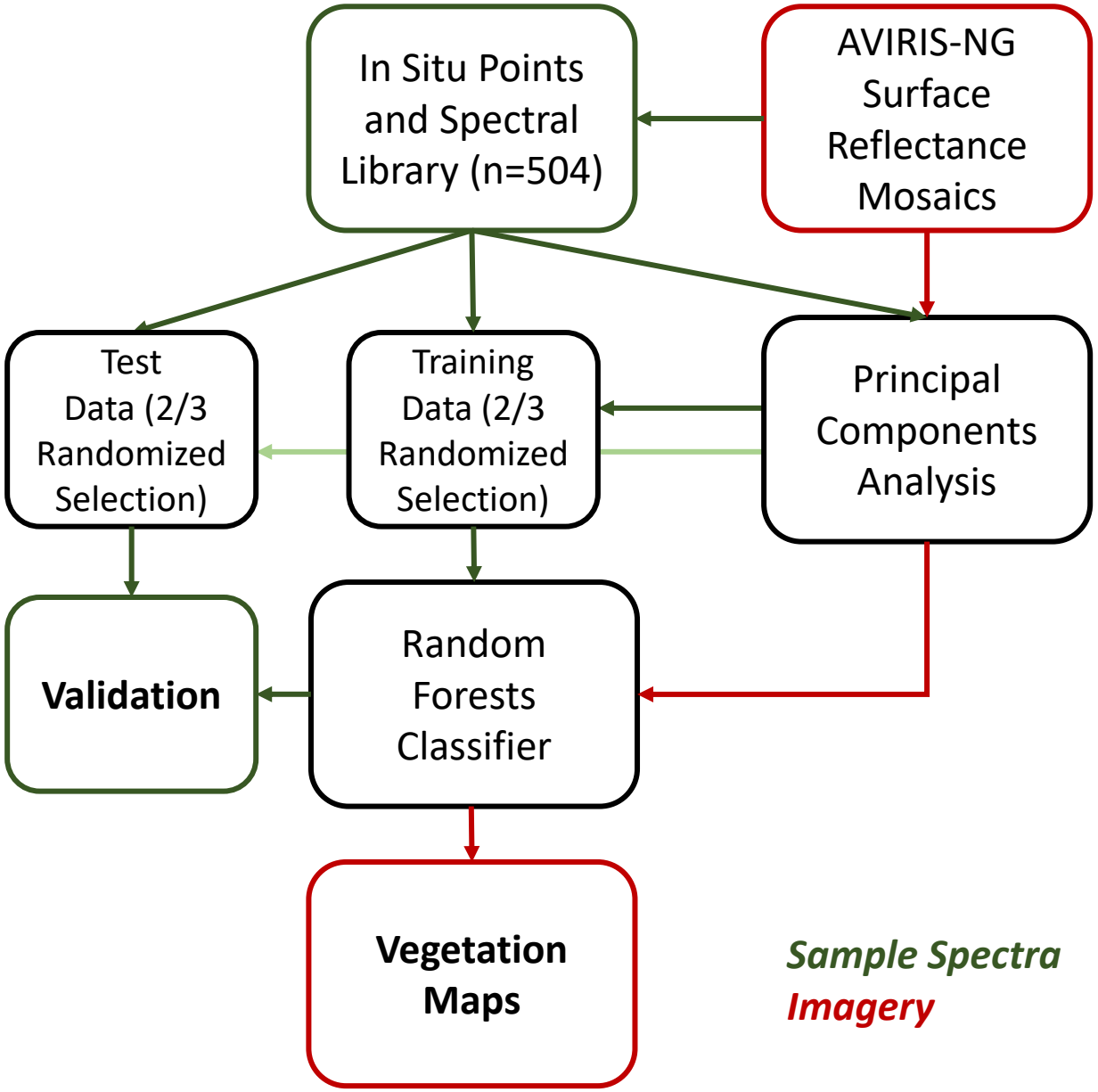

Classification Algorithm

- Principal Component Analysis (PCA) for dimension reduction calculated from spectral library (n=504)
  - Applied to mosaic imagery, selected PCs for classification inputs
    - Excised PCs with excess noise and discrepancies across flightlines
  - 13 final components, 99.86% variance explained

- Random Forests Classification model
  - Trained on 2/3 randomized selection of points within each class
  - Input data = 13 PCs

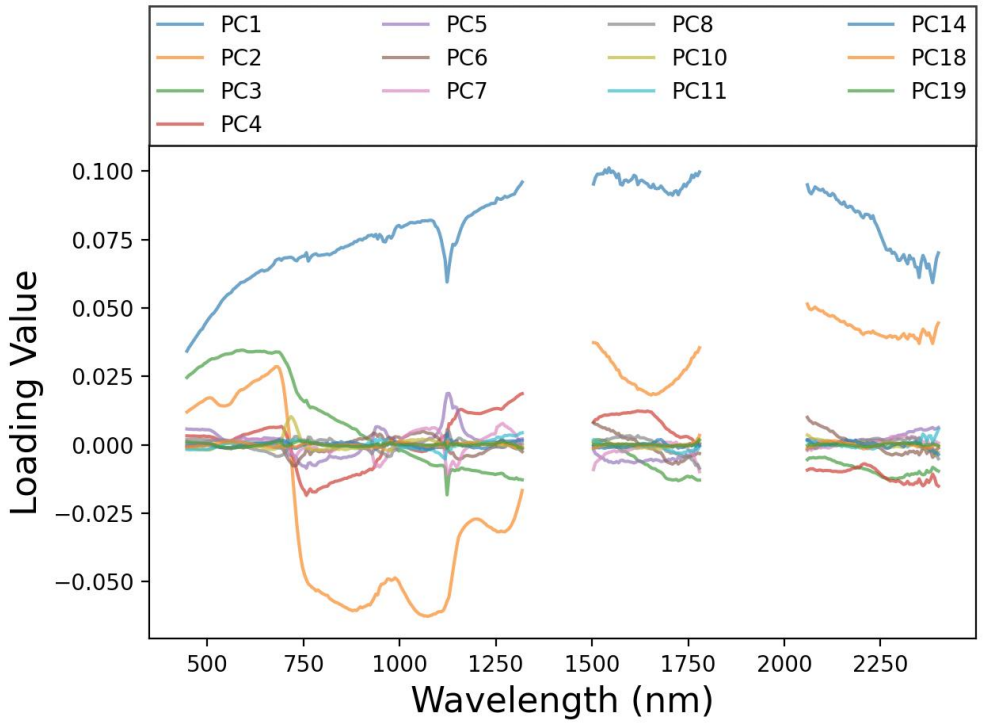

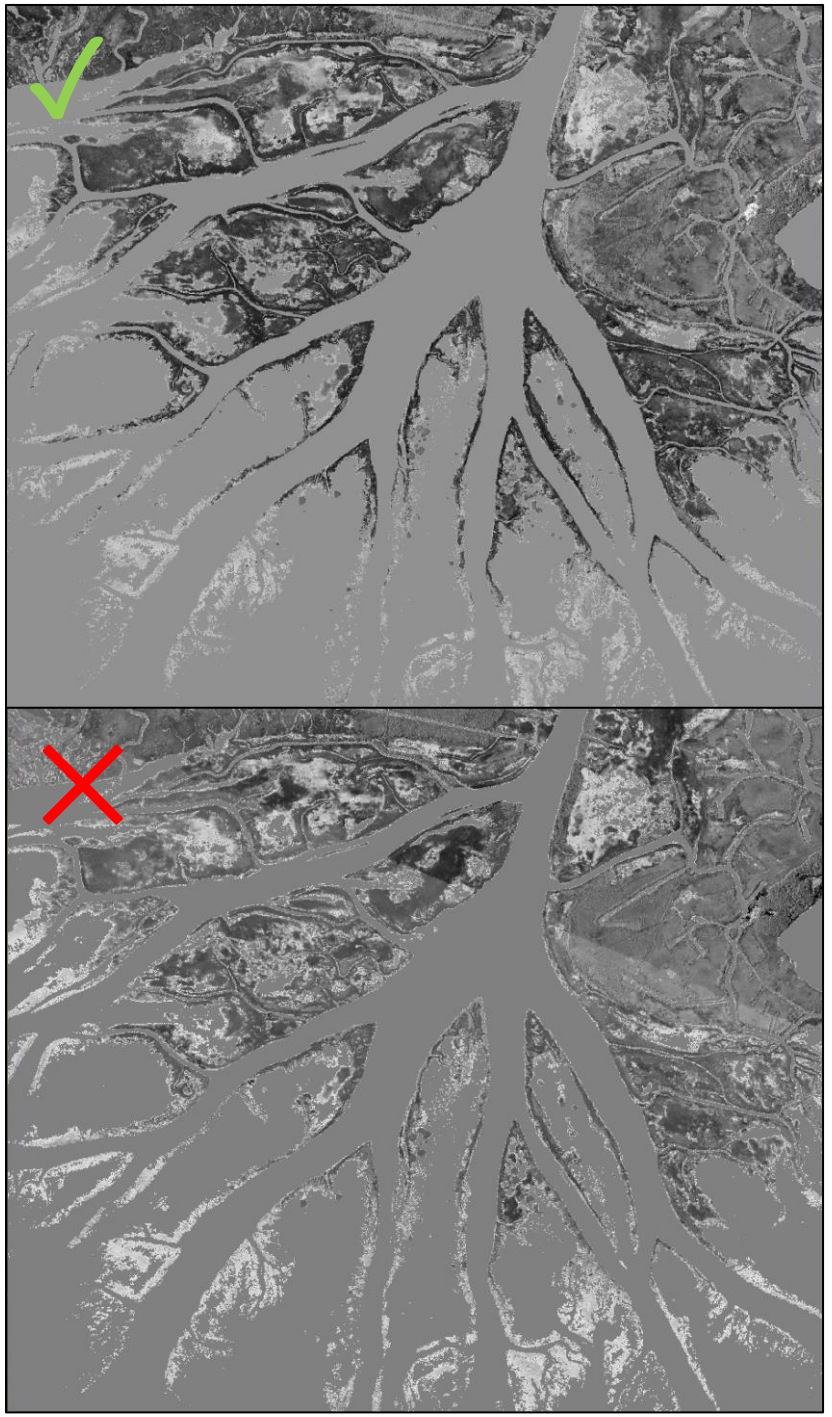

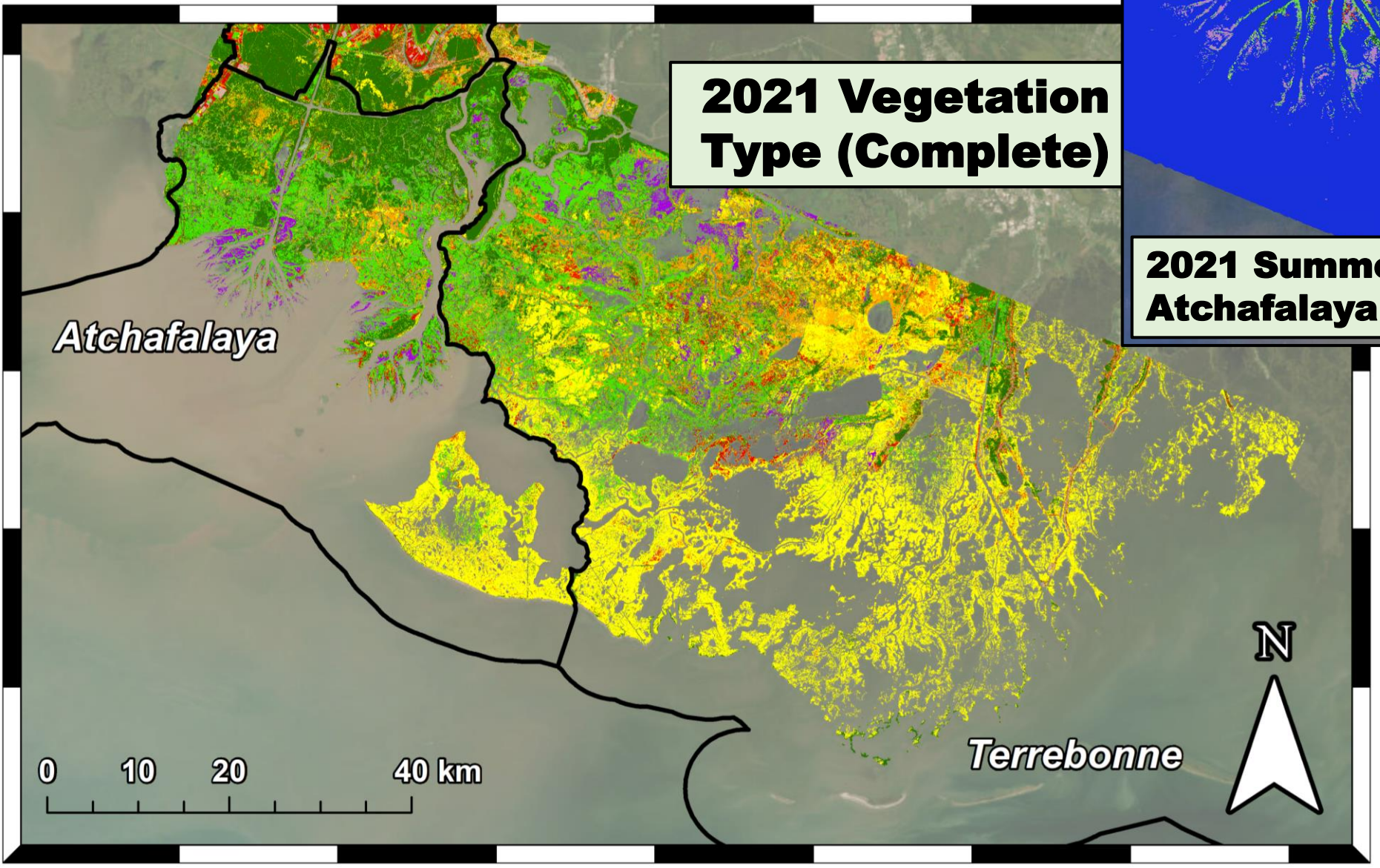

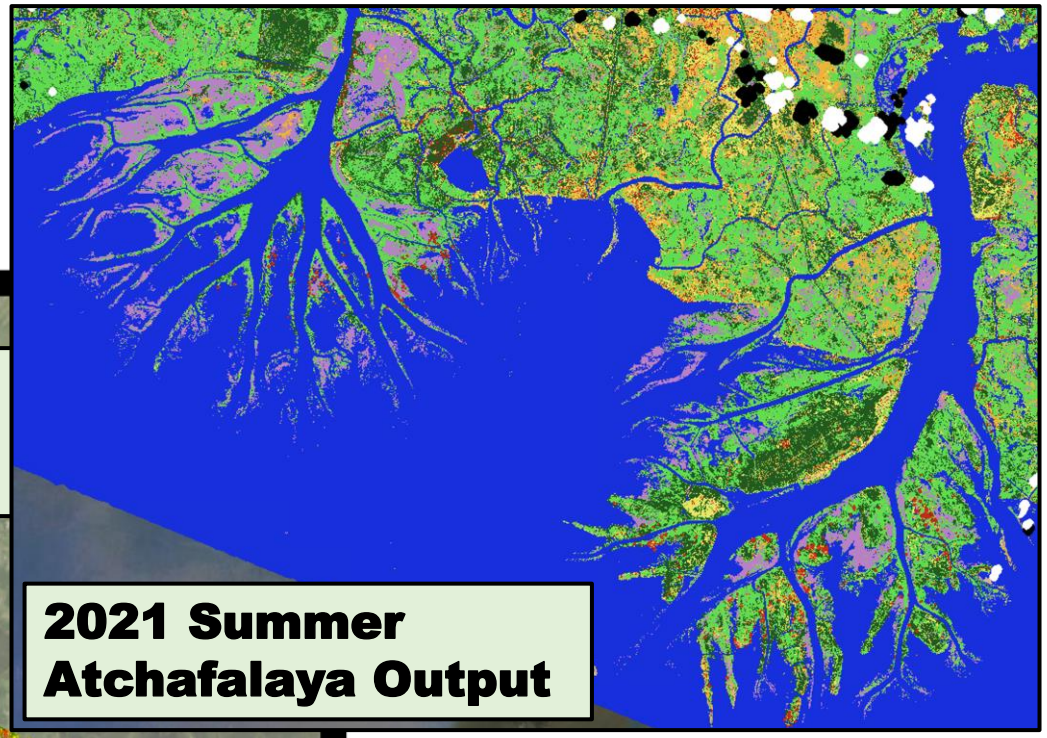

Water
Forest
Broadleaf Herbaceous
Freshwater Grass
Saltmarsh Grass
Tall Grasses
Aquatic Vegetation
Soil/Mudflat

Vegetation Map Validation

Validation Data Confusion Matrix		Reference Data							
		Forest	**Broadleaf Herbaceous**	**Freshwater Grass**	**Saltmarsh Grass**	**Tall Grasses**	**Aquatic**	**Soil/ Mudflat**	**All**
Classification Data	**Forest**	**16**	1	0	1	1	0	0	19
	Broadleaf Herbaceous	0	**12**	2	1	0	2	0	17
	Freshwater Grass	1	3	**14**	3	0	0	0	21
	Saltmarsh Grass	0	0	0	**57**	0	0	0	57
	Tall Grasses	0	0	2	5	**18**	0	0	25
	Aquatic	0	2	0	0	0	**11**	0	13
	Soil/Mudflat	0	0	0	1	0	0	**14**	15
	All	17	18	18	68	19	13	14	**167**

- 1/3 of each class's samples randomly selected for validation
- **Overall Accuracy: 0.85**
- **Overall Kappa: 0.81**

Aboveground Biomass (AGB) Algorithm

- Model herbaceous AGB as a function of reflectance spectra
  - Paired AGB samples + pixel spectra (April n=42, August n=42)
  - Noise artifacts remaining at 880-1000, 1080-1200 nm
    - Atmospheric water vapor absorption limiting signal from plant canopy water content
    - Conditional Gaussian interpolation algorithm over noisy bands using EMIT spectral library
  - Random Forests regression model
  - Jensen et al. (*in review*)

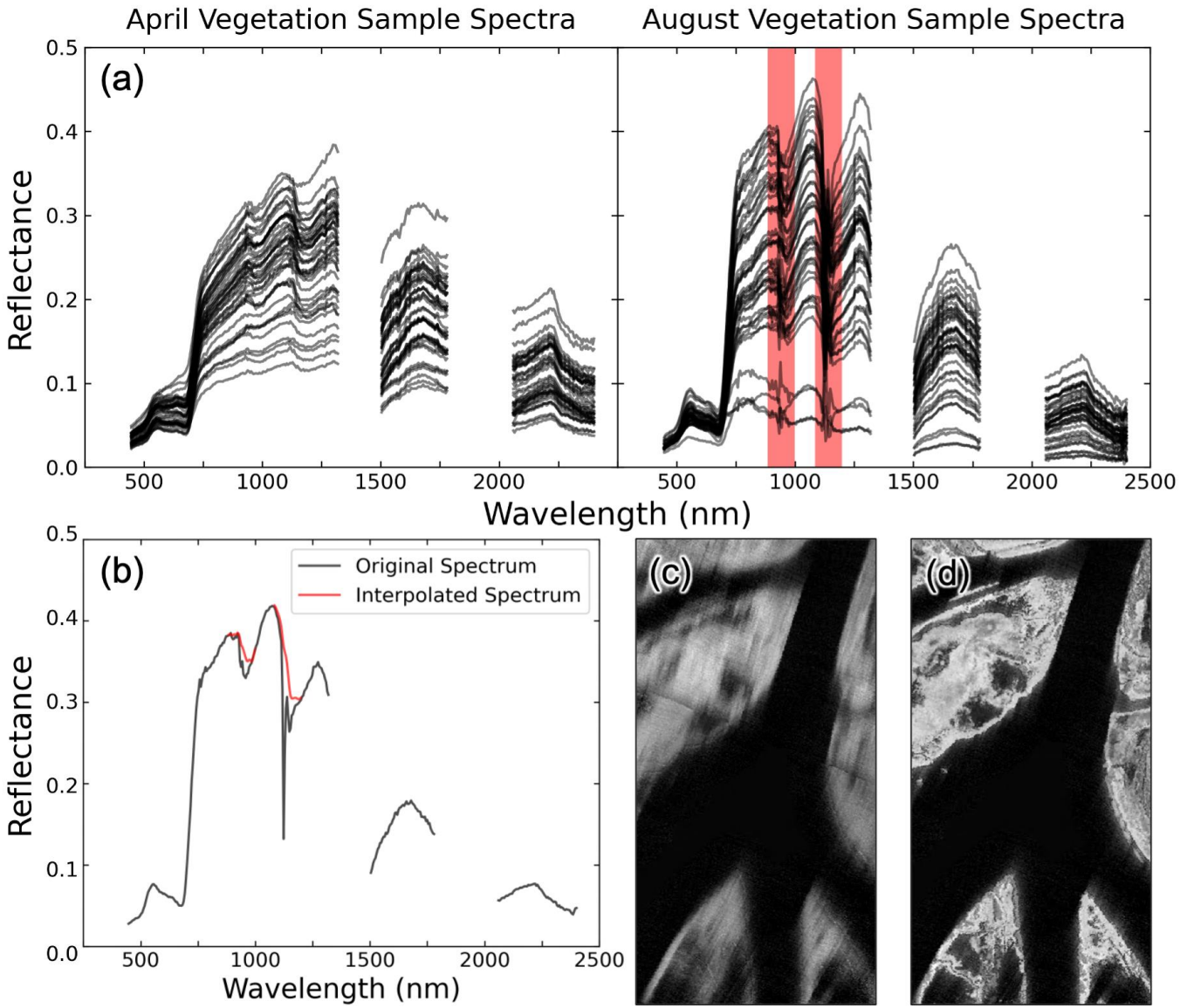

Model Comparisons

a) Uncorrected Partial Least Squares Regression

b) Corrected Partial Least Squares Regression

c) Corrected Random Forests Regression

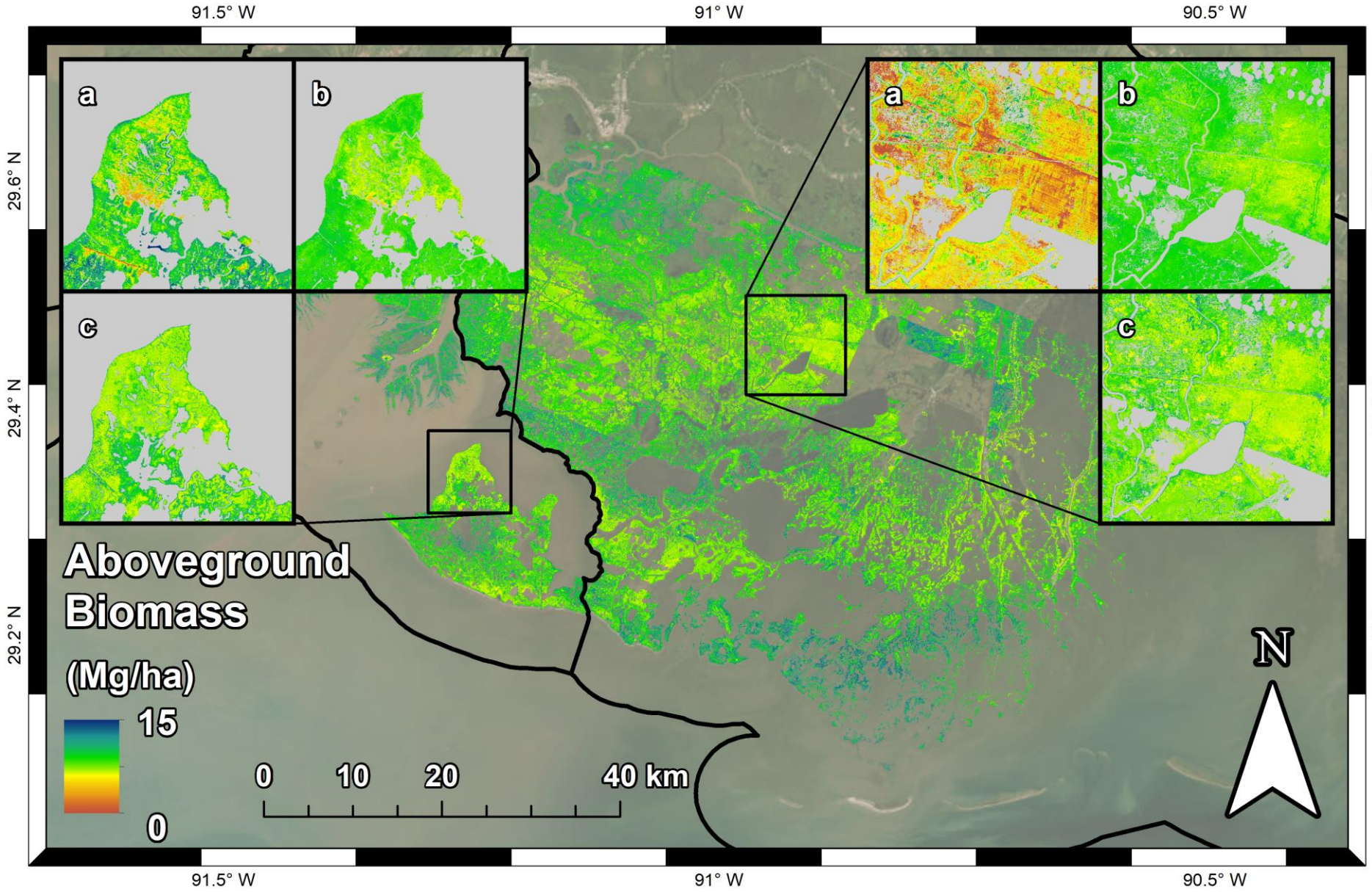

Herbaceous AGB Products

- Random Forests AGB model
  - R^2 = 0.89
  - MAE = 109.30 g/m^2
  - RMSE = 146.08 g/m^2
- Leave-One-Out Cross-Validation
  - R^2 = 0.43
  - MAE = 257.30 g/m^2
  - RMSE = 333.12 g/m^2

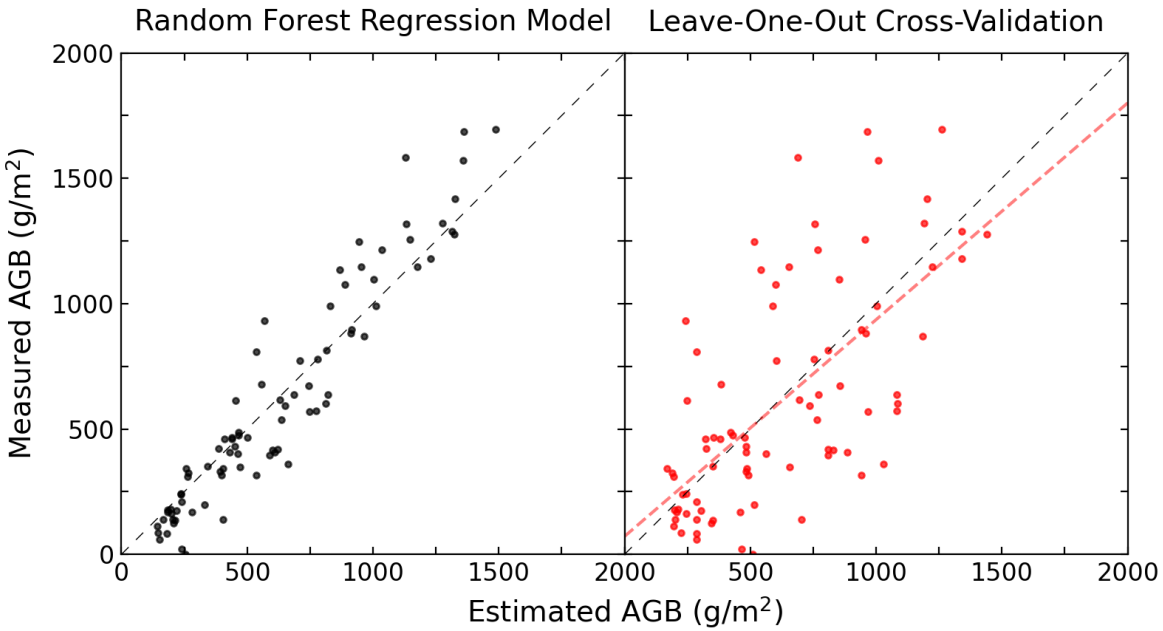

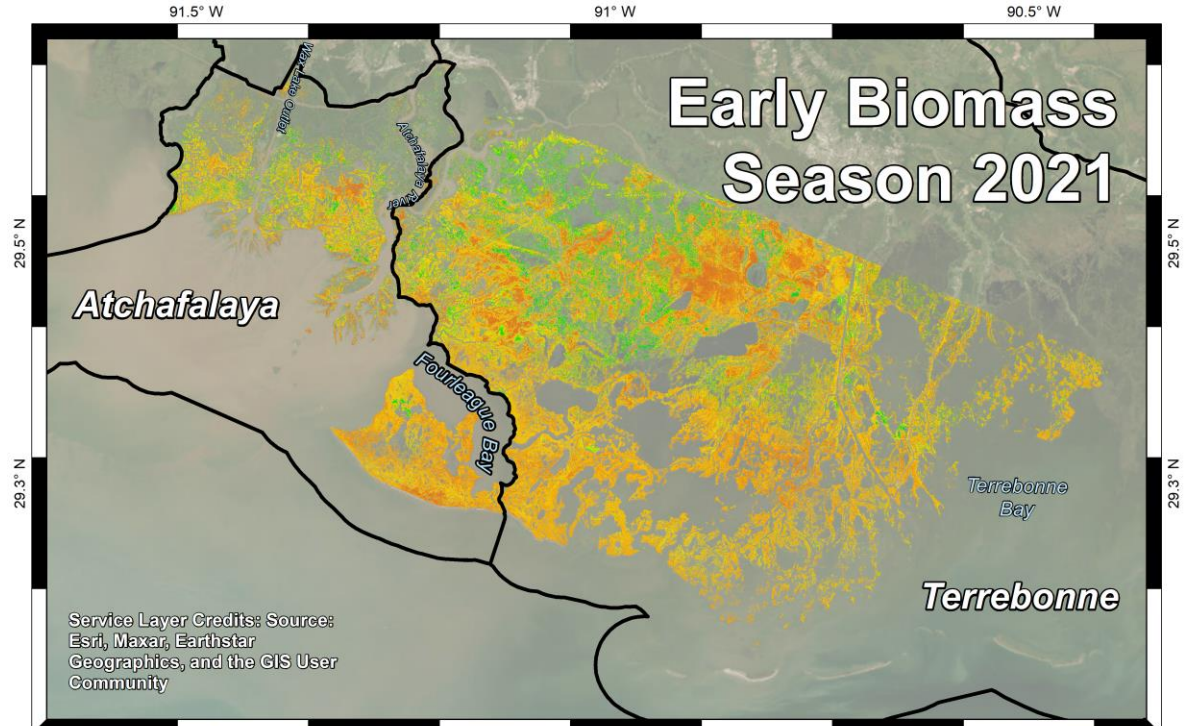

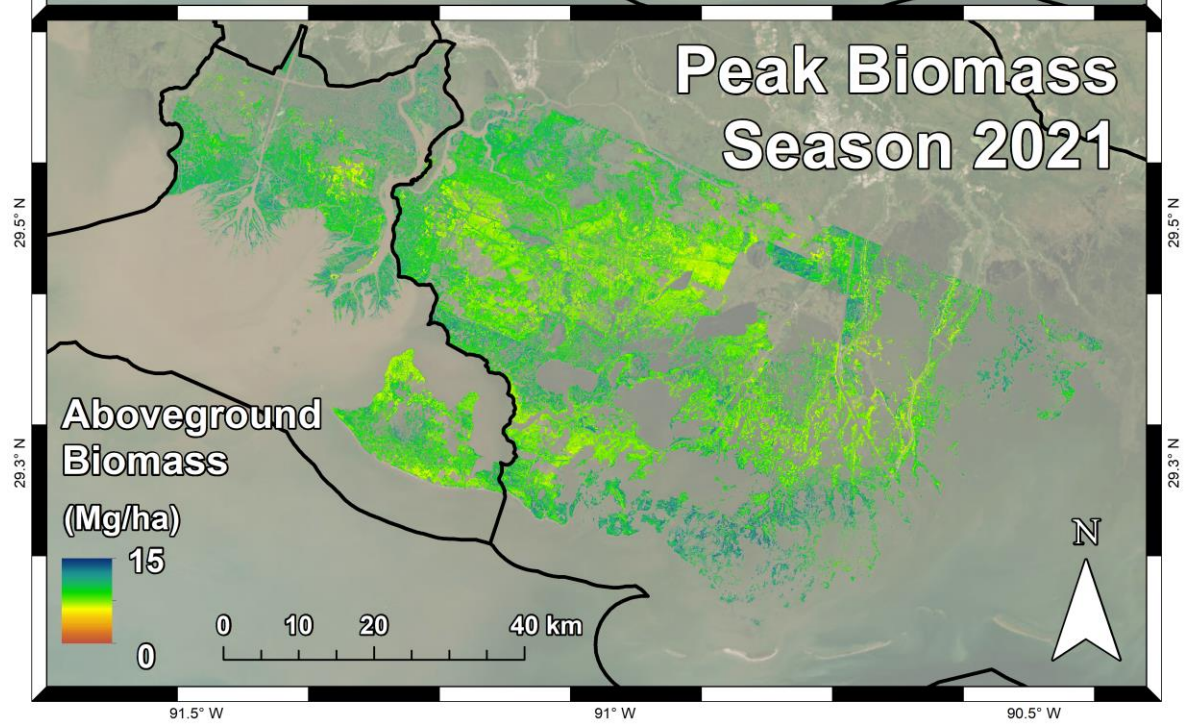

Acknowledgements

- Delta-X, Jet Propulsion Laboratory, California Institute of Technology
  - deltax.jpl.nasa.gov

Datasets

- Jensen, D.J., E. Castañeda-Moya, E. Solohin, A. Rovai, D.R. Thompson, and M. Simard. 2023. Delta-X: AVIRIS-NG L3 Derived Aboveground Biomass, MRD, Louisiana, USA, 2021, V2. ORNL DAAC, Oak Ridge, Tennessee, USA. https://doi.org/10.3334/ORNLDAAC/2138
- Thompson, D.R., D.J. Jensen, J.W. Chapman, M. Simard, and E. Greenberg. 2022. Delta-X: AVIRIS-NG BRDF-Adjusted Surface Reflectance, MRD, LA, 2021. ORNL DAAC, Oak Ridge, Tennessee, USA. https://doi.org/10.3334/ORNLDAAC/2025
- Castañeda-Moya, E., and E. Solohin. 2022. Delta-X: Aboveground Biomass and Necromass across Wetlands, MRD, Louisiana, 2021. ORNL DAAC, Oak Ridge, Tennessee, USA. https://doi.org/10.3334/ORNLDAAC/2000

References

- Chapman, John W., David R. Thompson, Mark C. Helmlinger, Brian D. Bue, Robert O. Green, Michael L. Eastwood, Sven Geier, Winston Olson-Duvall, and Sarah R. Lundeen. "Spectral and radiometric calibration of the next generation airborne visible infrared spectrometer (AVIRIS-NG)." *Remote Sensing* 11, no. 18 (2019): 2129.
- Greenberg, E., D. R. Thompson, D. J. Jensen, P. A. Townsend, N. Queally, A. Chlus, C. G. Fichot, J. Harringmeyer, and Marc Simard. "An improved scheme for correcting remote spectral surface reflectance simultaneously for terrestrial BRDF and water-surface sunglint in coastal environments." *Journal of Geophysical Research: Biogeosciences*.
- Jensen, D., Thompson, D.R., Simard, M., Solohin, E., & Castañeda-Moya, E. (*in review*). Imaging spectroscopy-based aboveground biomass and carbon estimation in Louisiana's coastal wetlands: Towards consistent spectroscopy for retrievals across atmospheric states. Submitted to Remote Sensing of Environment.
- Queally, Natalie, Zhiwei Ye, Ting Zheng, Adam Chlus, Fabian Schneider, Ryan P. Pavlick, and Philip A. Townsend. "FlexBRDF: A flexible BRDF correction for grouped processing of airborne imaging spectroscopy flightlines." Journal of Geophysical Research: Biogeosciences 127, no. 1 (2022).
- Thompson, D.R., Leifer, I., Bovensmann, H., Eastwood, M., Fladeland, M., Frankenberg, C., Gerilowski, K., Green, R.O., Kratwurst, S., Krings, T. and Luna, B., 2015. Real-time remote detection and measurement for airborne imaging spectroscopy: a case study with methane. Atmospheric Measurement Techniques, 8(10), pp.4383-4397.
- Thompson, D.R., Natraj, V., Green, R.O., Helmlinger, M.C., Gao, B.C. and Eastwood, M.L., 2018. Optimal estimation for imaging spectrometer atmospheric correction. Remote sensing of environment, 216, pp.355-373.
- Thompson, D.R., Cawse-Nicholson, K., Erickson, Z., Fichot, C.G., Frankenberg, C., Gao, B.C., Gierach, M.M., Green, R.O., Jensen, D., Natraj, V. and Thompson, A., 2019. A unified approach to estimate land and water reflectances with uncertainties for coastal imaging spectroscopy. Remote Sensing of Environment, 231, p.111198.
- Thompson, D.R., Braverman, A., Brodrick, P.G., Candela, A., Carmon, N., Clark, R.N., Connelly, D., Green, R.O., Kokaly, R.F., Li, L. and Mahowald, N., 2020. Quantifying uncertainty for remote spectroscopy of surface composition. Remote Sensing of Environment, 247, p.111898.